Reprinted from

Tenth International Symposium

Machine Processing of

Remotely Sensed Data

with special emphasis on

Thematic Mapper Data and

Geographic Information Systems

June 12 - 14, 1984

Proceedings

Purdue University
The Laboratory for Applications of Remote Sensing
West Lafayette, Indiana 47907 USA

ADAPTIVE FILTERING AND IMAGE SEGMENTATION FOR SAR ANALYSIS

D.G. GOODENOUGH, B. GUINDON, J.-F. MEUNIER

Canada Centre for Remote Sensing
Ottawa, Ontario, Canada

N.A. SWANBERG

Intera Technologies, Ltd.
Ottawa, Ontario, Canada

ABSTRACT

Classification by fields or homogeneous regions can be more accurate for agricultural applications than per pixel classifiers. Fields or segments are separated by boundaries. For an operational remote sensing system, such boundaries will likely be derived from the images themselves. The action of separating an image into homogeneous segments is called segmentation. Because of synthetic aperature radar (SAR) speckle, segmentation of SAR images has usually failed.

Using a SAR image acquired over Makofen, FDR with our Convair 580, we explore the effects of adaptive filter parameters, edge operators, and segmentation parameters on segmentation. The adaptive filter employed is an implementation of the Kansas filter (Frost, 1981), and is used at window sizes of 5x5, 7x7, 11x11 pixels over digitally processed, one look, X-band (VV), 5m pixel imagery. The edge operators used include Sobel, Laplacian, Robert's 2, and variance within an edge window of 3 by 3 pixels.

The segmentation program employed uses a graph-theoretic approach to identify homogeneous segments with inputs of the edge image and a smoothing parameter which is an estimate of the noise in the edge image. Since noise in a SAR image is multiplicative, unlike visible/IR imagery, some error can result from an improper choice of the smoothing parameter. We are presently searching for a more adaptive, smoothing parameter.

Following segmentation, the resulting segments in each image are compared to a manually defined edge image. A supervised classification of the segments is performed using the Euclidean distance between the segment means and those of a training set.

*With Intera Technologies Limited

I. INTRODUCTION

Synthetic aperture radar (SAR) imagery is noisy due to coherent speckle. In the past, this multiplicative noise has prevented us from successfully dividing a SAR image into homogeneous regions based upon the image intensities. We have tried to use median filtering to reduce speckle but this filter was not sufficient to produce an image which could be segmented. The application area was agriculture crop classification. For SAR imagery, we have found that pixel classification was necessary. For visible/IR imagery, our image segmentation algorithms were very effective.

In this paper we report on a new approach to image segmentation where we have used adaptive filtering to reduce noise in a SAR image. We have obtained our best SAR image segmentation to date by the methodology described herein. Further work is required to extend the techniques to segments with boundaries of low separability. A segmentation algorithm with an adaptive threshold for noise in the edge image will be required to obtain an image segmentation of quality comparable to a visible/IR image.

Section 2.0 contains a description of the test data set; section 3.0 describes the analysis methodology; section 4.0 gives the results; and section 5.0 summarizes our conclusions.

II. TEST DATA

The image selected for this study is an airborne SAR (X_{VV}) image, 256 by 256 pixels, which was digitally processed by the CCRS Generalized SAR Processor (GSAR), (Princz, 1983), to provide a 5 meter resolution, one-look, digital image. The grey levels in this 8-bit image are directly proportional to the square root of intensity (figure 2.1), thus giving grey levels with a more Gaussian distribution.

This image, selected for its varied segment size and brightness, covers a 1.28km x 1.28km area near Makofen in the Federal Republic of Germany. It is an agricultural site comprised of sugar beet, wheat, winter barley, potato, mixed hay and summer wheat, and corn fields (figure 2.2). The topography is relatively flat, with elevation variations of less than 8 meters about a mean of 344 meters above sea level.

Reference data for this site were collected by CCRS and German Aerospace Research Establishment (DFVLR) personnel during the week of July 4-11, 1981. Imagery over this site was acquired on July 6, 1981 with the CCRS Convair 580 as part of the European SAR 580 Campaign.

III. ANALYSIS

Following image selection, analysis was carried out at CCRS using the LANDSAT-4 Digital Image Analysis System (LDIAS), (Goodenough, 1983), and the CCRS Image Analysis System (CIAS), (Goodenough, 1979). First, a noise reducing filter was applied to the image. Since noise in SAR imagery is multiplicative rather than additive, as is the case with visible/IR imagery, an adaptive filter designed to reduce multiplicative noise while preserving edges within the image was used. The level of spatial averaging performed by this filter is a function of the mean squared to variance ratio within the filter window (Frost, 1981). Filtering was performed using three window sizes: 5x5, 7x7, and 11x11 (figures 3.1-3.3). Edge operators were then applied to the three resulting filtered images and the initial unfiltered image.

Four edge operators were employed:

Laplace (1)

$$L = I_{i}+1,j + I_{i}-1,j + I_{i},j+1 + I_{i},j-1 - 4I_{i},j$$

Roberts Distance Measure 2 (2)

$$R = \left|I_{i},j + 1 - I_{i},j-1\right| + \left|I_{i}+1,j - I_{i}-1,j\right|$$

(Gonzales et al, 1977)

Sobel (3)

$$S = \sqrt{(W_1^{\,2} + W_2^{\,2})}$$

where $W_1 = (I_{i}-1,j+1 + 2I_{i},j+1 + I_{i}+1,j+1\ )-$

$(I_{i}-1,j-1 + 2I_{i},j-1 + I_{i}+1,j-1\ )$

$W_2 = (I_{i}+j,j-1 + 2I_{i}+1,j + I_{i}+1,j+1\ )-$

$(I_{i}-1,j-1 + 2I_{i}-1,j + I_{i}-1,j+1\ )$

(Duda et al, 1971)

Variance in a 3 x 3 window (4)

(Sachs, 1982)

These four operators were applied to each of the four images resulting in 16 edge images on which segmentation was performed.

The segmentation algorithm employed uses a modified graph-theoretic approach, first advanced by Narendra and Goldberg (1980). These modifications ensure that a plateau between an edge image peak and valley will not be erroneously regarded as a "valley" by the algorithm. Inputs to this program include an edge image and a smoothing parameter which is a measure of noise tolerance for identifying an edge.

In order to determine which combination of adaptive filter window size and edge operator had produced the best segmentation, segmentation performance was evaluated only on those edges that were most readily apparent to the human observer. These edges were manually defined by two researchers independently. The resulting images agreed within one pixel and included 41 boundaries. Since the manually defined images were in such close agreement, one was arbitrarily chosen and used as reference against which the segmentations were compared (figure 3.4).

So that a quantitative measure of test boundary separability could be obtained, each of these boundaries was assigned a separability measure defined as:

$$S = \frac{\Delta I}{\sqrt{(\sigma_1^{\,2} + \sigma_2^{\,2})}}$$

where:

ΔI = the change in mean intensity across a field boundary

$\sigma_1^{\,2}$ = within field variance on either side of the boundary

Separability measures were computed with data from the unfiltered image. Separabilities of the test boundaries were compared.

Three criteria were used to evaluate the performance of the segmentation. First, it was determined whether or not all the manually defined boundaries were present in the segmentation. At this level of performance evaluation, spurious boundaries were ignored.

Since some of the segmented images contained thousands of segments, it was difficult to determine merely by examination, whether or not the boundaries being tested for were present (figure 3.5). To alleviate this problem, a mask was created.

The manually defined edge image was used to create the mask. The segment lines in the manually defined edge image were thickened so that each boundary in the mask represented the manually defined edge ±2 pixels (figure 3.6). This widening of the boundaries by ±2 pixels was done to allow for error in boundary placement that might have occurred in the segmentation due to noise remaining in the SAR image. Mask boundary pixels were given a value of one while the remaining mask pixels were assigned a value of zero.

Each of the segmented images were multiplied by this mask so that the product was an image where only the segment lines falling on the mask boundary pixels remained. From these images it was easy to determine which boundaries had been correctly delineated by a particular segmentation and which had not. Each of these images were examined to determine how many of the 41 boundaries were identified. Only segment boundaries that were continuous were counted (figure 3.7).

The second criterion used to evaluate segmentation performance was the total number of segments created within known bright homogeneous regions. Segments within eleven fields were counted in each image. Segmentations where these fields were broken into the fewest number of segments were considered to be the best.

Finally, a segment classifier was used to classify the selected segmented image. The algorithm used performs a supervised classification by computing the Euclidean distance between the segment means and those of a training set. The classification was compared to the reference data.

IV. RESULTS

Separabilities of the 41 test boundaries ranged from 0.3-1.5. Cases, in which segmentations produced using a smoothing parameter of zero delineated at least 20 test boundaries, were examined. 38% of the test boundaries in these images had separabilities of <1.0, however, as these images were segmented with an increased smoothing parameter, 87% of the test boundaries that dropped out had separabilities of <1.0.

Initially, the segmentation program was run using the 16 edge images and a smoothing parameter of zero. In some cases, this resulted in segmented images with nearly 6,000 segments. Having that number of segments in a 256 x 256 pixel image, we hypothesized, implied a high probability of finding test segment boundaries by chance. To test this hypothesis, four of the edge images, each having been created with one of the four edge operators and a 5 x 5 adaptive filter, were used.

Successive runs of the segmentation program were made on each image. The smoothing parameter was increased on each run until a smoothing parameter that produced a segmented image with between 1500- 2500 segments was reached. Again, the smoothing parameter was increased on successive runs until a smoothing parameter, producing a segmented image with less than 1,000 segments was found. This process resulted in 12 segmented images, three for each edge image (figure 4.1).

The pixels and lines in each of these images were then switched so that they bore no relation to the original SAR image. They were then multiplied by the mask and the resulting images were examined to determine how many of the 41 test boundaries were present merely by chance. The results are presented in Table 4.1 and show that, as expected, the number of boundaries present was related to the total number of segments. With less than 2,500, 1-4 segments could be expected to be found by chance. From this point in the investigation on, only segmented images with less than 2,500 segments were considered so as to avoid confusing edges that were "identified" by chance with those delineated by the segmentation algorithm.

Next, successive runs of the segmentation program were made using each of the 16 edge images and increasing the smoothing parameter until a segmented image for each, exhibiting less than 2,500 segments had been produced. These images were each multiplied by the mask and the resulting images were examined to determine how many of the 41 test boundaries were present. The results are presented in Table 4.2. So few boundaries were identified in the segmentations resulting from edge images that had been produced using an unfiltered image or the Laplacian edge operator, that these seven images were eliminated from further evaluation. With the limit on the number of segments, the remaining nine images were examined to determine the total number of segments created within 11 bright homogeneous fields for each image. The results are presented in Table 4.3. The segmentation produced from the 11 x 11 adaptive filtered, variance edge image created significantly fewer segments within the homogeneous regions. The total number of segments created, 703, was also much less than the upper limit of 2,500 segments (Figure 4.1).

The total number of segments created for the remaining eight segmented images was much higher than the 703 segments created in the 11 x 11, adaptive filtered, variance case. The total number of segments for these images ranged from 1559 to 2426. All eight segmentations had delineated between 28 and 34 of the 41 test boundaries. It was not known, however, how well the eight edge images, which had originally been segmented to produce at most 2,500 segments, would perform if they were segmented to produce at least 703 segments.

Successive runs of the segmentation program were made on each of the eight edge images. On each run, the smoothing parameter was increased until a segmentation yielding closest to, but not less than, 703 segments was achieved for each of the eight images. These images were then multiplied by the mask and the resulting images were examined to determine how many of the 41 test boundaries were present. The results are presented in Table 4.4 and show that the number of boundaries identified decreased significantly in those cases where the Sobel and Roberts 2 edge operators were used, but not in the instances where the variance edge operator was employed.

Since the variance, 7 x 7 and 11 x 11 cases performed comparably in terms of number of boundaries delineated, the number of segments within the eleven homogeneous areas for each were compared. The segmentation produced in the 7 x 7, variance case created 470 segments in the homogeneous areas while the 11 x 11 variance case created only 404 segments.

Finally, the 11 x 11 variance case, with its low number of spurious segments in the known homogeneous regions, was used with the segment classifier to classify the original SAR image. Figure 4.2 shows the classification results. The reference data is illustrated in Figure 2.2. Using the classified image and reference data, a confusion matrix was generated on a per pixel basis (Table 4.5). Over 1000 samples were taken for each class. Sugar beets, wheat, winter barley, and potatos were correctly classified 81%, 87%, 80% and 47% of the time, respectively.

V. DISCUSSION AND CONCLUSIONS

An investigation has been conducted to evaluate the effects of adaptive filtering and edge operators on SAR image segmentation and classification. Combinations of adaptive filter window sizes and edge operators were tested. A graph-theoretic segmentation algorithm was employed. The 11 x 11 adaptive filter and the variance edge operator in combination with the segmentation algorithm produced the segmented image exhibiting the greatest number of test boundaries while creating the fewest number of spurious segments within the known homogeneous regions.

A separability measure was used to obtain a quantitative measure of test boundary separability. A test boundary with a separability value of <1.0 was more likely to drop out as the segmentation smoothing parameter was increased. This separability measure may prove useful in subsequent studies when comparing segmentation from different SAR scenes with the same resolution. One factor that appears to affect boundary delineation is boundary length. This factor is not currently included in our separability measure and is an area where further research is needed.

The selected segmented image was classified. An algorithm which performs a supervised classification computing the Euclidean distance between the segment means and those of a training set was used. A confusion matrix was generated on a pixel by pixel basis. Sugar beets, wheat, winter barley, and potatoes were correctly classified 81%, 87%, 80%, and 47% of the time respectively. The poor classification accuracy obtained for potatoes is due to the fact that potatoes were frequently misclassified as sugar beets.

These results can be compared to results from a different area in the same image where maximum likelihood classification was previously performed. Prior to classification, a 3 x 3 median filter was applied to this 10 m resolution data. Sugar beets, wheat, winter barley, and potatoes had classification accuracies of 80%, 69%, 61%, and 56% respectively using this per pixel classifier. Thus, classification accuracies for wheat and barley appear to increase substantially when an adaptive filter and a segment classifier are used.

Segment classification errors resulted from two basic problems. In the first case, a field was not delineated as a distinct segment. Instead, its pixels were included in a segment with an adjacent, often larger field of another crop type. As all pixels in a segment are assigned to a single class, the pixels in the smaller field were often misclassified. In order to reduce errors of this type, the initial edge detection and segmentation must be improved. Though adaptive filtering substantially improves segmentation results for SAR images, more research is needed to delineate boundaries of low separability. Our future research will include efforts to implement a gap filling routine and add an adaptive smoothing parameter to the segmentation algorithm currently in use.

In the second case, fields were delineated as separate segments, but the segments were misclassified. This is not a reflection on success of segmentation, but indicative of class overlap. This study was conducted on a single band of SAR data. We anticipate that as we add more bands and different polarizations, these classification errors may decrease, and boundaries may be more easily delineated resulting in better segmentation.

Table 4.1. Number of Boundaries Identified by Chance as Related to Total Number of Segments

EDGE OPERATOR	SMOOTHING PARAMETER	TOTAL NUMBER OF SEGMENTS	NUMBER OF TEST BOUNDARIES IDENTIFIED
Laplacian	0	5975	25
Roberts 2	0	4570	17
Sobel	0	4246	17
Variance	0	2623	4
Laplacian	12	2427	1
Roberts 2	3	2136	4
Variance	1	1773	4
Sobel	9	1732	2
Sobel	12	984	0
Roberts 2	5	934	0
Laplacian	24	857	0
Variance	3	644	0

Table 4.2. Numbers of Detected Test Boundaries
(maximum of 2500 segments;
total of 41 boundaries)

		ADAPTIVE FILTER SIZE		
EDGE OPERATOR	UNFILTERED	5 x 5	7 x 7	11 x 11
Sobel	13	32	34	29
Variance	14	27	33	32
Roberts 2	8	28	32	34
Laplace	4	10	9	17

Table 4.3. Total Numbers of Segments Within 11 Bright Homogenous Regions

EDGE OPERATOR	ADAPTIVE FILTER SIZE 5 x 5	7 x 7	11 x 11
Sobel	1019	996	1004
Variance	916	1157	404
Roberts 2	974	1238	1188

Table 4.4. Numbers of Detected Boundaries (smoothing parameter selected to locate at least 703 segments)

EDGE OPERATORS	ADAPTIVE FILTER SIZE 5 x 5	7 x 7	11 x 11
Sobel	17	22	20
Variance	25	31	32
Roberts 2	15	22	26

Table 4.5. Confusion Matrix - Reference Classes Across vs. Classification Down as Percentage of Classification

	SUGAR BEETS	WHEAT	WINTER BARLEY	POTATO
SUGAR BEETS	81.05 %	0.00 %	0.02 %	51.23 %
WHEAT	0.00 %	87.41 %	18.85 %	0.62 %
WINTER BARLEY	0.74 %	12.24 %	80.52 %	0.66 %
POTATO	18.16 %	0.35 %	0.61 %	47.35 %
OTHER CLASSES	0.05 %	0.00 %	0.00 %	0.14 %
UNCLASSIFIED	0.00 %	0.00 %	0.00 %	0.00 %

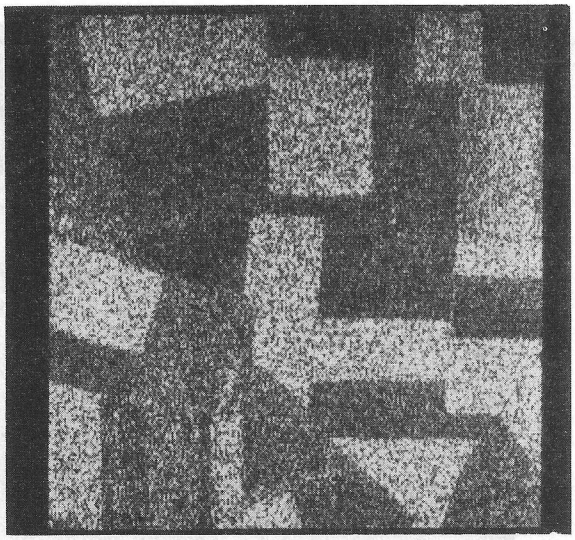

Figure 2.1 Airborne SAR (X_{VV}) Image of Study Site.

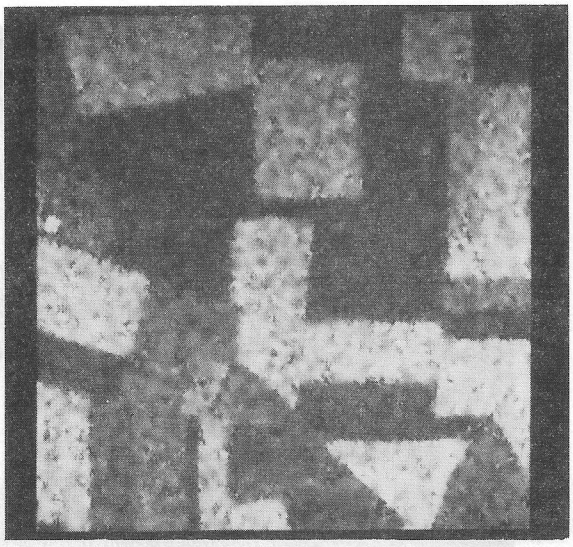

Figure 3.1 5x5 Adaptive Filtered SAR Image.

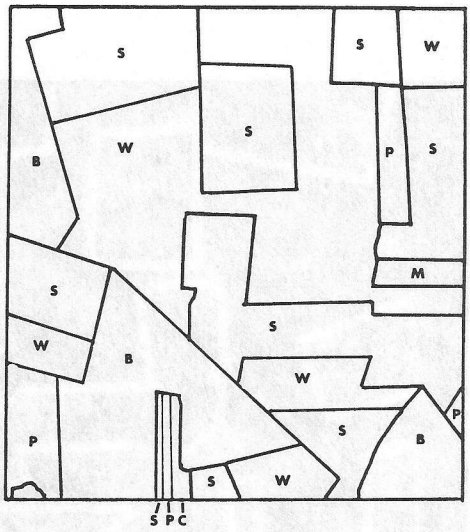

S - sugar beets
W - wheat
B - winter barley
P - potatoes
C - corn
m - mixed hay and summer wheat

Figure 2.2 Reference Data.

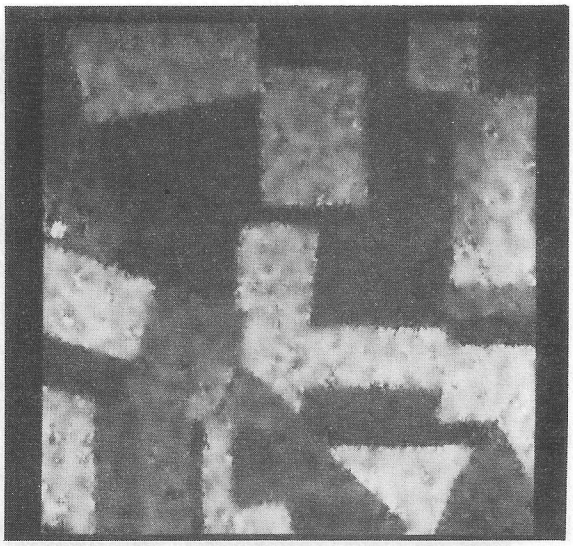

Figure 3.2 7x7 Adaptive Filtered SAR Image.

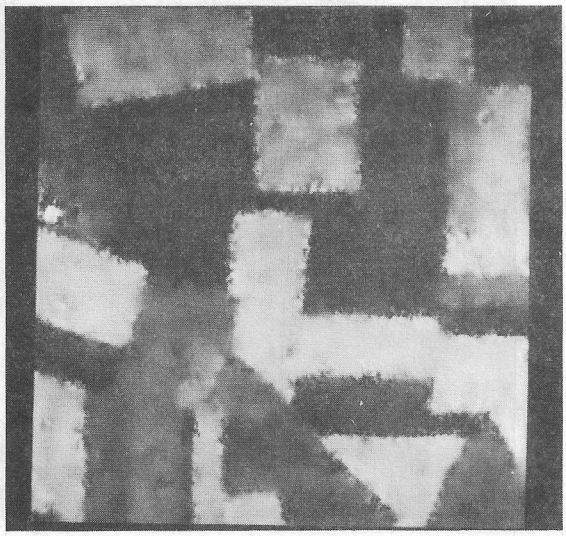

Figure 3.3 11x11 Adaptive Filtered SAR Image.

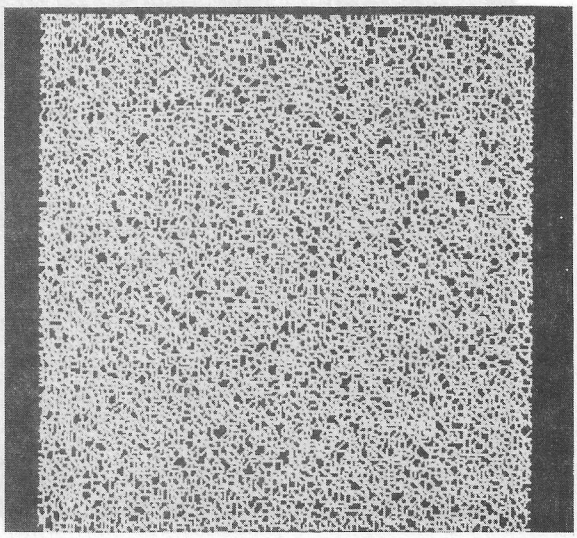

Figure 3.5 Segmented Image Containing Thousands of Segments.

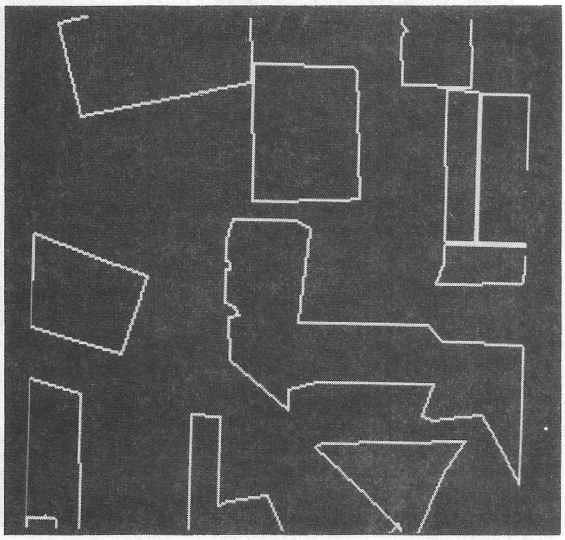

Figure 3.4 Manually Defined Edges.

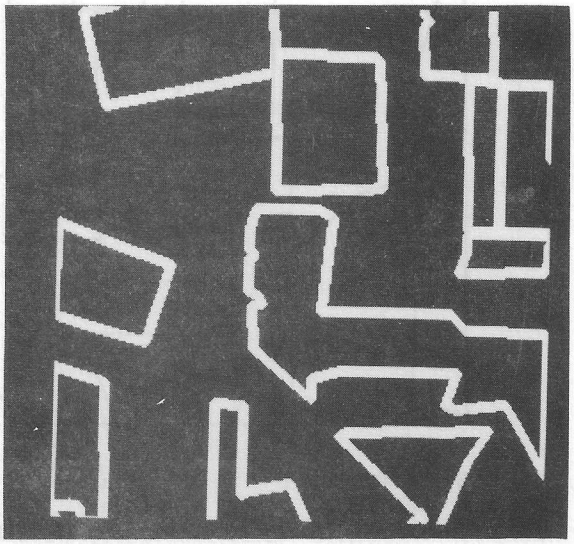

Figure 3.6 Manually Defined Edge Image ± 2 Pixels.

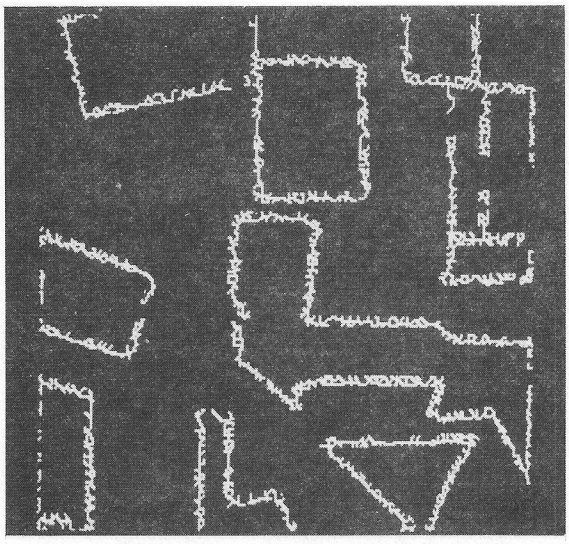

Figure 3.7 Product of the Mask and a Segmentation.

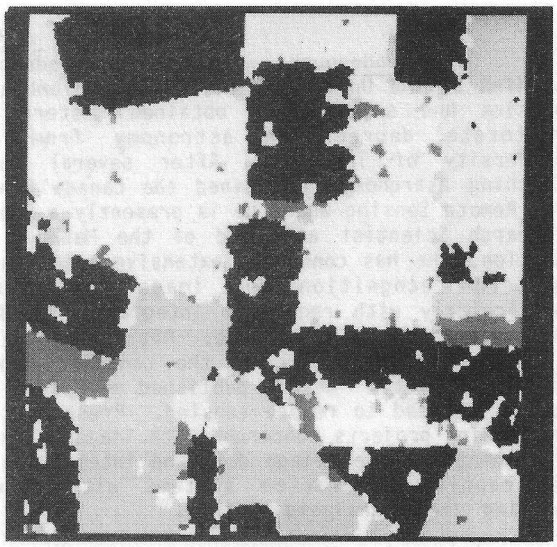

Figure 4.2 Classified Image.

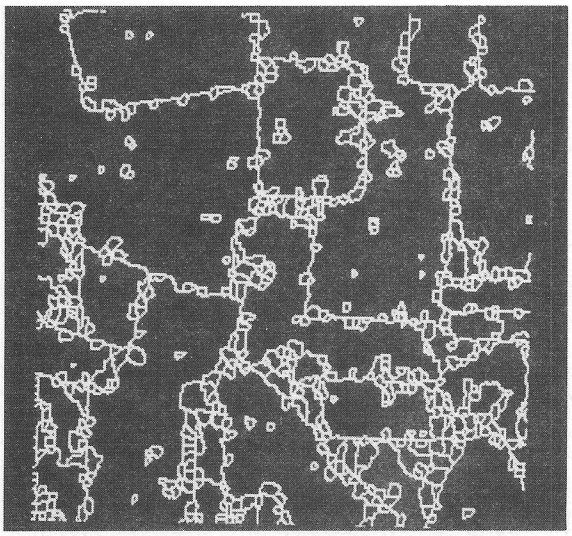

Figure 4.1 Segmented Image Produced With 11x11 Adaptive Filter and Variance Edge Operator.

VI. ACKNOWLEDGEMENTS

The authors would like to thank David Kell for his work on implementing the adaptive filter.

VII. REFERENCES

Duda, R.O. and P.E. Hart, 1971, Pattern Classification and Scene Analysis, Wiley, New York.

Gonzales, R.C., and P. Wincz, 1977, Digital Image Processing, Addison- Wesly Publishing Co., Inc., Reading, Mass.

Goodenough, D.G., 1979, 'The Image Analysis System (CIAS) at the Canada Centre for Remote Sensing', Canadian Journal of Remote Sensing, Vol. 5, No. 1.

Goodenough, D.G., 1983, 'A New Image Analysis System for LANDSAT-4 Thematic Mapper Data', presented at the VIII Canadian Symposium on Remote Sensing, Montreal, P.Q.

Narendra, P.M. and M. Goldberg, 1980, 'Image Segmentation with Directed Trees', IEEE Transactions on Pattern Analysis and Machine Intelligence, Vol. PAMI-2, No. 2.

Princz, J., 1983, 'CCRS Digitally Processed Image Products', Proceedings of the Eighth Canadian Symposium on Remote Sensing.

Sachs, L., 1982, Applied Statistics, Springer-Verlag, New York.

D.G. Goodenough. Dr. David Goodenough studied at the University of British Columbia in physics and subsequently obtained Masters and Doctorate degrees in astronomy from the University of Toronto. After several years teaching astronomy, he joined the Canada Centre for Remote Sensing where he is presently a Senior Research Scientist and Head of the Methodology Section. He has conducted extensive research in pattern recognition and image processing, particularly with regard to integration of data from aircraft and satellites. Dr. Goodenough is a member of the IEEE and the Canadian Remote Sensing Society. He has published more than 60 papers related to remote sensing. Presently, he is leading projects concerned with image analysis of thematic mapper image data and integration of geographic information systems with remote sensing image analysis systems.

B. Guindon. Dr. Bert Guindon is a Research Scientist with the Canada Centre for Remote Sensing. He received a Doctorate in Physics from Queen's University in 1976. Since joining CCRS in 1978, he has been actively involved in a variety of image processing projects. His primary research interests include geometric correction and digital SAR image analysis.

N.A. Swanberg. Nancy Swanberg is a Research Assistant with Intera Technologies, Ltd. She received a B.S. in Forestry from Southern Illinois University in 1980 and an M.S. in Natural Resources/Remote Sensing in 1981 from the University of Michigan. Since joining Intera in 1982, she has been on contract to the Canada Centre for Remote Sensing. She has been involved in a wide variety of image analysis research at CCRS and is currently pursuing segmentation of digital SAR and Thematic Mapper data.

J.-F. Meunier. Jean-François Meunier received a B.A.Sc. in Electrical Engineering from the University of Ottawa in 1977. After two years of graduate studies and research assistantship in digital image processing at the University of Ottawa, he worked as a research assistant for Intera Environmental Consultants Limited on contract to the Canada Centr for Remote Sensing. He is now a Physical Scientist with CCRS working in image analysis and pattern recognition.